

Chuang Wen
Yuying Yan *Editors*

Advances in Heat Transfer and Thermal Engineering

Proceedings of 16th UK Heat Transfer
Conference (UKHTC2019)

 Springer

Advances in Heat Transfer and Thermal Engineering

Chuang Wen · Yuying Yan
Editors

Advances in Heat Transfer and Thermal Engineering

Proceedings of 16th UK Heat Transfer
Conference (UKHTC2019)

 Springer

Editors

Chuang Wen
Faculty of Engineering
University of Nottingham
Nottingham, UK

Yuying Yan
Faculty of Engineering
University of Nottingham
Nottingham, UK

ISBN 978-981-33-4764-9

ISBN 978-981-33-4765-6 (eBook)

<https://doi.org/10.1007/978-981-33-4765-6>

© Springer Nature Singapore Pte Ltd. 2021

This work is subject to copyright. All rights are reserved by the Publisher, whether the whole or part of the material is concerned, specifically the rights of translation, reprinting, reuse of illustrations, recitation, broadcasting, reproduction on microfilms or in any other physical way, and transmission or information storage and retrieval, electronic adaptation, computer software, or by similar or dissimilar methodology now known or hereafter developed.

The use of general descriptive names, registered names, trademarks, service marks, etc. in this publication does not imply, even in the absence of a specific statement, that such names are exempt from the relevant protective laws and regulations and therefore free for general use.

The publisher, the authors and the editors are safe to assume that the advice and information in this book are believed to be true and accurate at the date of publication. Neither the publisher nor the authors or the editors give a warranty, expressed or implied, with respect to the material contained herein or for any errors or omissions that may have been made. The publisher remains neutral with regard to jurisdictional claims in published maps and institutional affiliations.

This Springer imprint is published by the registered company Springer Nature Singapore Pte Ltd.

The registered company address is: 152 Beach Road, #21-01/04 Gateway East, Singapore 189721, Singapore

Preface

Nowadays, we are facing ever-severe crisis of conventional energy resources and pollutions, increasing demand for new energy resources and applications, and significant challenges for the technologies of efficient cooling, heat and mass transfer enhancement, and effective thermal management, etc. These have become crucially important for almost all engineering area and industries such as mechanical, aerospace, civil and building, chemical and process, electric and electronic, pharmaceutical and medical, as well as power industries.

Over the more than 100 years development, heat transfer has now become a cross-disciplinary subject. The study on micro-nano scale heat transfer has played an important role in the research progress of material science, and the development of biomedical engineering, etc. The 16th UK Heat Transfer Conference (UKHTC2019) addressed these challenges. The conference gathered the UK active and leading researchers typically many young and new academic colleagues, as well as the researchers from heat transfer communities of Europe, North Americans, Australia, South Africa, Kuwait, Japan, and China, etc.

The conference was aimed at a closer collaboration and cooperation between the UK and international scholars in the field of heat transfer. The UK National Heat Transfer Committee organised this conference biennially to provide an innovative platform for scholars in thermal engineering to share and exchange new ideas and solutions. Six plenary and three keynote lectures and more than 190 papers were presented at UKHTC2019 throughout two days in four sets of seven parallel oral sessions. The proceedings in the title of *Advances in Heat Transfer and Thermal Engineering* contains selected and the authors agreed extended abstracts or papers that cover almost all the topics in heat transfer and thermal engineering.

We would like to thank all authors for their contributions to UKHTC2019 and thank the staff members of the University of Nottingham to provide active assistance during the preparation stage of this conference. We send our sincere gratitude to the dedicated reviewers for their time and contribution to improve the scientific quality of the manuscripts. We also would like to acknowledge the support received from the sponsors. We hope that the emerging solutions described in the conference

proceedings will inspire our academic and industrial communities to create, innovate, and build a more energy-efficient world.

Nottingham, UK

Chuang Wen
Yuying Yan

Contents

Convection

Natural Convection from Heated Surface-Mounted Circular Cylinder	3
H. Malah, Y. S. Chumakov, and S. Ramzani Movafagh	
Experimental Investigation of Transitional Flow Forced Convection Heat Transfer Through a Smooth Vertical Tube with a Square-Edged Inlet	9
Abubakar I. Bashir, Marilize Everts, and Josua P. Meyer	
Effects of Rarefied Effect, Axial Conduction, and Viscous Dissipation on Convective Heat Transfer in 2D Parallel Plate Microchannel or Nanochannel with Walls at Uniform Temperature	15
Qiangqiang Sun, Kwing-So Choi, and Xuerui Mao	
Enhancement of Laminar Natural Convection Heat Transfer in Horizontal Annuli Using Two Fins	23
A. El Amraoui, A. Cheddadi, and M. T. Ouazzani	
A Computational Study of Ultrasound-Enhanced Convective Heat Transfer	29
Raheem Abbas Nabi, Yi Sui, and Xi Jiang	

Boiling-Evaporation-Condensation

Wall Effects on the Thermocapillary Migration of Single Fluorinert Droplet in Silicon Oil Liquid	37
Yousuf Alhendal and Ali Turan	
Modelling of Flash Boiling in Two-Phase Geothermal Turbine	45
S. Rane and L. He	
Experimental Investigation on Flash Evaporation of Pure Water at Different Depths with Functional Analysis Method	51
Siguang Li, Yanjun Li, Longbin Yang, Xiaojin Zhang, and Runzhang Xu	

Investigation on the Characteristics of Droplet Evaporation Under Different Heating Conditions Using Lattice Boltzmann Method	55
Li Wang, Yuying Yan, and Nick Miles	
Evaporating Progress of Hexane Droplet on the Surface of NaCl Solution	59
Bin Liu, Ruonan Wang, Georges El Achkar, and R. Bennacer	
Numerical Simulation on Heat Transfer Characteristics of Steam-Water Two-Phase Flow in Smooth Tube and Rifled Tube	63
Wanze Wu, Baozhi Sun, Jianxin Shi, Xiang Yu, and Zhirui Zhao	
Lubrication Model for Vapor Absorption/Desorption of Hygroscopic Liquid Desiccant Droplets	67
Zhenying Wang, George Karapetsas, Prashant Valluri, Khellil Sefiane, and Yasuyuki Takata	
Fixation of Thermocouples and Insulation for Heated Block	71
Viktor Vajc and Martin Dostál	
Droplet Interplay on Microdecorated Substrates	79
Veronika Kubyshkina, Khellil Sefiane, Daniel Orejon, and Coinneach Mackenzie Dover	
Effect of Inlet Subcooling on Flow Boiling Behaviour of HFE-7200 in a Microchannel Heat Sink	83
Vivian Y. S. Lee, Gary Henderson, and Tassos G. Karayiannis	
Heat Transfer Measurements for Condensation of FC72 in Microchannels	89
Lei Chai, Jiong Hui Liu, Nan Hua, Guang Xu Yu, John W. Rose, and Hua Sheng Wang	
Bubble Dynamics and Heat Transfer on Biphilic Surfaces	93
P. Pontes, R. Cautela, E. Teodori, A. S. Moita, A. Georgoulas, and António L. N. Moreira	
Molecular Dynamics Simulation of Effect of Temperature Difference on Surface Condensation	99
J. H. Pu, Q. Sheng, J. Sun, W. Wang, and H. S. Wang	
The Strong Influence of Thermal Effects on the Lifetime of an Evaporating Droplet	105
Feargus G. H. Schofield, Stephen K. Wilson, David Pritchard, and Khellil Sefiane	
Coupled Water and Ethanol Vapour Transfer to and from Volatile Ethanol Drops in Humid Air: Diffusion Model Revisited	111
Yutaku Kita, Daniel Orejon, Yasuyuki Takata, and Khellil Sefiane	

Significantly Enhanced Pool Boiling Heat Transfer on Multi-walled Carbon Nanotubes Self-assembly Surface 115
 Lan Mao, Wenbin Zhou, Xuegong Hu, Yu He, and Rong Fu

Heat Transfer Analysis of a Tubular Solar Still Considering the Non-uniform Temperature Distribution on the Condensing Shell 121
 Tiantong Yan, Guo Xie, and Licheng Sun

Droplet Deposition Pattern Affected by Heating Directions 125
 Zeyu Liu, Yuying Yan, Xinyong Chen, Li Wang, and Xin Wang

Effect of Vapour Pressure on Power Output of a Leidenfrost Heat Engine 131
 Prashant Agrawal, Gary G. Wells, Rodrigo Ledesma-Aguilar, Glen McHale, Anthony Buchoux, Khellil Sefiane, Adam Stokes, Anthony J. Walton, and Jonathan G. Terry

Three-Dimensional Computer Simulation of Heat Flux-Controlled Pool Boiling of Water-Based Nanofluids by the Coupled Map Lattice Method 137
 Asheesh Kumar and Partha Ghoshdastidar

Heat Transfer of Condensing Saturated and Non-saturated Hydrocarbons Inside Horizontal Tubes 143
 S. Fries and A. Luke

Analysis of the Influence of Thermophysical Properties on the Coupled Heat and Mass Transfer in Pool Boiling 147
 Niklas Buchholz and Andrea Luke

Experimental Investigation of Various Influence Parameters on the Onset of Nucleate Boiling 151
 M. E. Newton, H. Margraf, J. Addy, and A. Luke

Study on Morphological Development of Fuel Droplets After Impacted on Metal Surfaces with Different Wettability 157
 Liang Guo, Gaofei Chen, Wanchen Sun, Degang Li, Yuheng Gao, and Peng Cheng

Optimizing the Design of Micro-evaporators via Numerical Simulations 163
 Mirco Magnini and Omar K. Matar

Simultaneous Laser- and Infrared-Based Measurements of the Life Cycle of a Vapour Bubble During Pool Boiling 169
 Victor Voulgaropoulos, Gustavo M. Aguiar, Matteo Bucci, and Christos N. Markides

Experimental Observations of Flow Boiling in Horizontal Tubes for Direct Steam Generation in Concentrating Solar Power Plants	175
Hannah R. Moran, Victor Voulgaropoulos, Dimitri Zogg, Omar K. Matar, and Christos N. Markides	
Multiscale Investigation of Nucleate Boiling and Interfaces	179
E. R. Smith, M. Magnini, and V. Voulgaropoulos	
Effect of Surface Wettability on Nanoscale Boiling Heat Transfer	183
Longyan Zhang, Jinliang Xu, Junpeng Lei, and Guanglin Liu	
Effect of Bulk Temperature on the Evaporation of a Nitrogen Drop in Different Immiscible Liquids	191
Neville Rebelo, Huayong Zhao, François Nadal, Colin Garner, and Andrew Williams	
CFD Modelling of Gas-Turbine Fuel Droplet Heating, Evaporation and Combustion	197
Mansour Al Qubeissi, Geng Wang, Nawar Al-Esawi, Oyuna Rybdylova, and Sergei S. Sazhin	
A Study of Nucleate Boiling Conjugate Heat Transfer	203
Robin Kamencky, Michael Frank, Dimitris Drikakis, and Konstantinos Ritos	
Flow Boiling of Water in a Square Metallic Microchannel	207
S. Korniliou, F. Coletti, and T. G. Karayiannis	
Experimental Study on Flow Boiling Heat Transfer of Refrigerant R1233zd in Microchannels	211
Xin Yu You, Jiong Hui Liu, Nan Hua, Ji Wang, Rongx Hui Xu, Guang Xu Yu, and Hua Sheng Wang	
Study on the Pool Boiling Bubble Departure Diameter and Frequency from Porous Graphite Foam Structures	217
I. Pranoto, K. C. Leong, A. A. Rofiq, H. M. Arroisi, and M. A. Rahman	
Investigation of Droplet Evaporation on Copper Substrate with Different Roughness	225
Xin Wang, Zeyu Liu, Li Wang, and Yuying Yan	
Enhanced Heat Transfer	
Enhance Heat Transfer and Mass Transfer in the Falling Film Absorption Process by Adding Nanoparticles	231
Hongtao Gao, Fei Mao, Yuchao Song, Jiaju Hong, and Yuying Yan	
Pulsating Heat Stripes: A Composite Polymer Sheet with Enhanced Thermal Conductivity	247
Oguzhan Der, Marco Marengo, and Volfango Bertola	

Study of Heat Transfer Enhancement by Pulsating Flow in a Rectangular Mini Channel 253
 Parth S. Kumavat, Richard Blythman, Darina B. Murray, and Seamus M. O’Shaughnessy

The Potential Use of Graphene to Intensify the Heat Transfer in Adsorption Beds 259
 Ahmed Rezk, Laura J. Leslie, and Rees Davenport

A Parametric Study into a Passively Enhanced Heat Separation System 265
 Chidiebere Ihekwaba and Mansour Al Qubeissi

Heat Transfer During Pulsating Liquid Jet Impingement onto a Vertical Wall 271
 J. Wassenberg, P. Stephan, and T. Gambaryan-Roisman

Icing of Water Droplet Enhanced with the Electrostatic Field 277
 Qiyuan Deng, Hong Wang, Xun Zhu, Qiang Liao, Rong Chen, and Yudong Ding

Micro-Nano Heat Transfer

Performance Enhancement of Vapour-Compression Refrigeration Systems Using Nanoparticles: An Experimental Study 283
 V. La Rocca, M. Morale, A. Ferrante, and A. La Rocca

Thermal Conductivity Correlation for Microscale Porous Media by Using OpenPNM 287
 Ángel Encalada, Mayken Espinoza-Andaluz, and Martin Andersson

Ethylene Glycol and Propanol: Understanding the Influence of an Extra Hydroxyl Group on the Mechanisms of Thermal Conductivity 293
 Likhith Manjunatha, Hiroshi Takamatsu, and James J. Cannon

Experimental Investigation of Thermal Performance and Liquid Wetting of a Vertical Open Rectangular Microgrooves Heat Sink with Fe₃O₄-Water Nanofluids 297
 R. Fu, W. B. Zhou, J. H. Wang, and X. G. Hu

On the Measurement Error of Temperature in Nanocomposite Thermal Insulation by Thermocouples 303
 Chao Fan, Xiao-Chen Zhang, Chuang Sun, and Xin-Lin Xia

Thermal Effect on Breakup Dynamics of Double Emulsion Flowing Through Constricted Microchannel 309
 Yong Ren, Yuning Huang, Yuying Yan, and Jing Wang

Design and Analysis of Synthetic Jet for Micro-channel Cooling	315
Ashish Mishra, Akshoy Ranjan Paul, Anuj Jain, and Firoz Alam	
Thermal Bioeffect of Hybrid Microfluidic System Used for Particle and Cell Separation	321
Ali Mohammad Yazdani, Hossein Alijani, Arzu Özbey, Mehrdad Karimzadehkhoei, Ali Koşar, Alper Şişman, Emre Alpman, and Rana Altay	
Computational Heat Transfer	
Numerical Simulation of Natural Convection in Solar Chimney	327
Hichem Boulechfar and Hadjer Bahache	
Numerical Investigation on Heat Transfer Performance of Triply Periodic Minimal Surface Structures for Supercritical CO₂ Cycles	331
Weihong Li, Guopeng Yu, and Zhibin Yu	
Temperature-Dependent Conductances to Improve the Accuracy of the Dynamic Model of an Electric Oven	335
Michael Lucchi, Nicola Suzzi, and Marco Lorenzini	
Numerical Simulation on Combustion Simulation Based on Soft-Measuring Technique	341
Yingai Jin, Mingyu Quan, Shijuan Yan, Yuying Yan, and Jiatong Guo	
Numerical Investigation of Mass Redistribution in Supercritical Water-Cooled Reactor Flow Channels	345
Zhirui Zhao, Yitung Chen, Baozhi Sun, Jianxin Shi, Xiang Yu, and Wanze Wu	
Numerical Study of the Impacts of Forced Vibration on Thermocapillary Bubble Migration in a Rotating Cylinder	349
Fatima Alhendal and Yousuf Alhendal	
Numerical Study on the Freezing Point of Methane Hydrate Dissociation by Depressurization	355
Qun Zhang, Longbin Yang, Yazhou Shao, Shidong Wang, and Runzhang Xu	
Multi-bubble Coalescence Simulations with Large Density Ratio Using Improved Lattice Boltzmann Method	361
Hongtao Gao, Xiupeng Ji, Jiaju Hong, Yuchao Song, and Yuying Yan	
A New Approach to Inverse Boundary Design in Radiation Heat Transfer	377
Mehran Yarahmadi, J. Robert Mahan, and Farshad Kowsary	
Numerical Investigation of Thermal Dynamic Response in Porous Media—A Pore-Scale Study	385
Rabeeah Habib, Bijan Yadollahi, and Nader Karimi	

Numerical Simulation of Thermal–Hydraulic Performance of a Round Tube-Fin Condenser with Liquid–Vapour Separation 391
 Nan Hua, Ying Chen, and Hua Sheng Wang

Numerical Modelling of Wet Steam Flows in Turbine Blades 397
 Chuang Wen, Xiaowei Zhu, Hongbing Ding, and Yan Yang

Evaluation of Neck Tissue Heat Transfer in Case of Stenosis in the Carotid Artery 403
 Ashish Saxena, Vedabit Saha, and E. Y. K. Ng

CFD-Enabled Optimization of Polymerase Chain Reaction Thermal Flow Systems 409
 Hazim S. Hamad, N. Kapur, Z. Khatir, Osvaldo Querin, H. M. Thompson, and M. C. T. Wilson

Modelling and Evaluation of the Thermohydraulic Performance of Finned-Tube Supercritical Carbon Dioxide Gas Coolers 417
 Lei Chai, Konstantinos M. Tsamos, and Savvas A. Tassou

Modeling Fouling Process on Tubes with Lattice Boltzmann Method and Immersed Boundary Method 423
 Zi-Xiang Tong, Dong Li, Ya-Ling He, and Wen-Quan Tao

Numerical Study of the Impacts of Forced Vibration on Thermocapillary Bubble Migration 427
 Mohammad Alhendal and Yousuf Alhendal

CFD Modelling and Experimental Calibration of Concentrated Windings in a Direct Oil-Cooled Segmented Stator 433
 Robert Camilleri

Numerical and Experimental Investigation on Single-Point Thermal Contact Resistance 439
 Anliang Wang, Zhenyu Liu, Hongwei Wu, Andrew Lewis, and Tahar Loulou

Optimization of Conformal Cooling Channels for Rapid Prototyped Mould Inserts 443
 Tongyan Zeng, James Jewkes, and Essam Abo-Serie

Numerical Analysis of a Segmented Annular Thermoelectric Generator 449
 Samson Shittu, Guiqiang Li, Xudong Zhao, and Xiaoli Ma

Heat Transfer Modelling of APAA Transmit-Receive Modules 455
 V. I. Zhuravliov, N. M. Naumovich, and V. S. Kolbun

Numerical Optimisation of the Regenerator of a Multi-stage Travelling Wave Thermoacoustic Electricity Generator 459
 Wigdan Kisha and David Hann

Experimental and Numerical Investigation of the Effects of Different Heat Transfer Modes on the Sublimation of Dry Ice in an Insulation Box	465
Abhishek Purandare and Srinivas Vanapalli	
Heat Transfer and Thermal Stress Analysis of PDC Cutter in Rock Breaking Process	469
Zengzeng Zhang, Yan Zhao, and Congshan Zhang	
Thermal Performance Evaluation Methodology of Grooved Heat Pipes with Rectangular, Trapezoidal and Wedge Cross Sections	475
Gökay Gökçe and Zafer Dursunkaya	
Thermal Management	
Development of High Heat Dissipation and Low Thermal Expansion Printed Wiring Boards	483
Yohei Ito and Sohei Samejima	
Optimization of Thermal Management of Li-Ion Cells with Phase Change Materials	487
S. Landini, R. Waser, A. Stamatou, J. Leworthy, J. Worlitschek, and T. S. O'Donovan	
The Simulation of the Motor Temperature Distribution with Spray Cooling	493
Xuehui Wang, Bo Li, and Yuying Yan	
Influence of Nanofluids Inlet and Outlet Positions on CPU Cooling Performance	497
Cong Qi, Jinghua Tang, Tiantian Chen, Maoni Liu, Guiqing Wang, and Yuying Yan	
The Temperature Uniformity Analysis and Optimization on the Lithium-Ion Battery with Liquid Cooling	505
Guohua Wang, Yuying Yan, and Qing Gao	
Heat Spreading Performance of Integrated IGBT Module with Bonded Vapour Chamber for Electric Vehicle	509
Bo Li, Yiyi Chen, Yuying Yan, Xuehui Wang, Yong Li, and Yangang Wang	
Predicting the Temperature Distribution in a Lithium-Ion Battery Cell for Different Cooling Strategies	517
Mahmoud Sawani and Robert Camilleri	
Electro-osmotic Non-isothermal Flow in Rectangular Channels with Smoothed Corners	521
Marco Lorenzini	

Transient Simulation of Finned Heat Sinks Embedded with PCM for Electronics Cooling 527
 Adeel Arshad, Pouyan Talebizadehsardari, Muhammad Anser Bashir, Muhammad Ikhlaiq, Mark Jabbal, Kuo Huang, and Yuying Yan

Experimental Investigation of Mini Pin-Fin Heat Sink Filled with PCM for Thermal Management 533
 Adeel Arshad, Luke Jackman, Mark Jabbal, and Yuying Yan

Experimental and Numerical Heat Transfer Investigation of Impingement Jet Nozzle Position in Concave Double-Wall Cooling Structures 537
 Edward Wright, Abdallah Ahmed, Yuying Yan, John Maltson, and Lynda Arisso Lopez

Critical Review and Ranking of Novel Solutions for Thermal Management in Electric Vehicles 543
 Marco Bernagozzi, Anastasios Georgoulas, Nicolas Miché, Cedric Rouaud, and Marco Marengo

System Simulation on the Refrigerant-Based Lithium-Ion Battery Thermal Management Technology 549
 Qing Gao, Ming Shen, and Yan Wang

Investigation on Battery Thermal Management Based on Phase Change Energy Storage Technology 553
 Hongtao Gao, Yutong Liu, Jiaju Hong, Yuchao Song, and Yuying Yan

Design and Simulation of the Thermal Management System for 5G Mobile Phones 563
 Zhaoshu Chen, Yong Li, Wenjie Zhou, and Yuying Yan

Investigation of Critical Overheating Behavior in Batteries for Thermal Safety Management 569
 Mengdi Zhao, Qing Gao, Tianshi Zhang, and Yubin Liu

Experimental Study on Direct Expansion Cooling Battery Thermal Management System 573
 Yuan Meng, Gao Qing, Zhang Tianshi, and Wang Guohua

Numerical Analysis of Thermal Systems of a Bus Engine 577
 Konstantinos Karamanos, Yasser Mahmoudi Larimi, Sung In Kim, and Robert Best

Robust Optimisation of Serpentine Fluidic Heat Sinks for High-Density Electronics Cooling 583
 Muyassar E. Ismaeel, N. Kapur, Z. Khatir, and H. M. Thompson

Numerical Study on the Fluid Flow and Heat Transfer Performance of Flat Miniature Heat Pipe for Electronic Devices Cooling 591
 Fei Xin, Ting Ma, Yuying Yan, and Qiuwang Wang

Thermal Performance on a Vapor Chamber-Based Battery Thermal Management System 597
 Dan Dan, Hongkui Lian, Yangjun Zhang, Yuying Yan, and Chengning Yao

Conformal Cooling of Aluminium Flat Fins Using a 3D Printed Water-Cooled Mould 603
 Y. Liang, R. Sharma, E. Abo-Serie, and J. Jewkes

A Hybrid Microchannel and Slot Jet Array Heat Sink for Cooling High-Power Laser Diode Arrays 609
 Zeng Deng, Jun Shen, Wei Dai, Ke Li, and Xueqiang Dong

Thermal Design for the Passive Cooling System of Radio Base Station with High Power Density 617
 Kai-Wen Duan, Ji-Wei Shi, and Wen-Quan Tao

Design and Experimental Study on a New Heat Dissipation Method for Watch-Phones 621
 Wenjie Zhou, Yong Li, Zhaoshu Chen, Yuying Yan, and Hanyin Chen

Heat Exchanger

Experimental and Numerical Investigation on Fouling and Heat Transfer Performance of a Novel H-type Finned Heat Exchanger 629
 Song-Zhen Tang, Zhan-Bin Liu, Ming-Jia Li, and Wen-Quan Tao

Improvement of Multi-objective Optimization Tool for Shell-and-Tube Heat Exchanger Design 635
 Thomas McCaughtry and Sung in Kim

Performance Analysis on Compact Heat Exchangers for Activated Carbon-Ethanol Adsorption Heat Pump/Thermal Storage 641
 Takahiko Miyazaki, Nami Takeda, Yuta Aki, Kyaw Thu, Nobuo Takata, Shinnosuke Maeda, and Tomohiro Maruyama

Experimental Validation of a Numerical Model of a Corrugated Pipe-Phase Change Material (PCM)-Based Heat Exchanger to Harness Greywater Heat 645
 Abdur Rehman Mazhar, Shuli Liu, and Ashish Shukla

Fluid Flow

A Heat Transfer Analysis of Separated and Reattached Flow Around a Heated Blunt Plate 653
 Christopher D. Ellis, Hao Xia, and Gary J. Page

Flow and Heat Transfer Characteristics of Piezoelectric-Driven Synthetic Jet Actuator with Respect to Their Stroke Length 659
 Muhammad Ikhlaiq, Mehmet Arik, Adeel Arshad, and Mark Jabbal

RANS Model Validation of Natural Circulation in Differentially Heated Cavities 663
 Constantinos Katsamis, Tim Craft, Hector Iacovides, and Juan Uribe

Experimental and Numerical Investigation of the Heat Transfer Characteristics of Laminar Flow in a Vertical Circular Tube at Low Reynolds Numbers 669
 Suvanjan Bhattacharyya, Marilize Everts, Abubakar I. Bashir, and Josua P. Meyer

The Role of Turbulence Models in Simulating Urban Microclimate 675
 Azin Hosseinzadeh, Nima shokri, and Amir Keshmiri

Temperature Effect on Falling Behaviour of Liquid Gallium Droplet ... 681
 M. Sofwan Mohamad, C. M. Mackenzie Dover, and K. Sefiane

Needle-Based Formation of Double Emulsion Encapsulating Multiple Cores in Parallel Mode 687
 Zheng Lian, Yong Ren, Kai Seng Koh, Jun He, George Z. Chen, Yuying Yan, and Jing Wang

Flow-Visualization Experimental Research on the Plume Pattern Above a Horizontal Heated Cylinder 691
 Guopeng Yu, Haiteng Ma, Weihong Li, Li He, and Zhibin Yu

Experimental Study of Thermal Field of a Pebble Bed Channel with Internal Heat Generation 695
 Meysam Nazari and Yasser Mahmoudi

Numerical Simulation for a Single Bubble on the Vertical Flat Surface by an Immiscible Two-Phase LBM 699
 Tomohiko Yamaguchi and Satoru Momoki

Experimental Study on Fuel Spray Impingement Process Against Metal Surface with Different Wettability 705
 Liang Guo, Jianyi Wei, Wanchen Sun, Xuejiang Hao, Deigang Li, and Kai Fang

Effect of Turbulence Models on Steam Condensation in Transonic Flows 711
 Chuang Wen, Nikolas Karvounis, Jens Honore Walther, Hongbing Ding, Yan Yang, Xiaowei Zhu, and Yuying Yan

An Experimental Study on Vent Locations in Road Racing Bicycle Helmet to Optimize Thermal Comfort and Aerodynamic Efficiency 717
 Harun Chowdhury, Firoz Alam, Terence Woo, and Akshoy Ranjan Paul

A Novel Horizontal Liquid–Liquid Flow Pattern Map Using Dimensionless Number Groups 721
 Olusegun Samson Osundare, Liyun Lao, and Gioia Falcone

Coupling Thermal–Fluid–Solid Modeling of Drilling Fluid Seepage into Coal Seam Borehole for CO₂ Sequestration 727
 Shu-Qing Hao

Simulation and Experimental Research on Flow Field and Temperature Field of Diamond Impregnated Drill Bit 733
 Baochang Liu, Shujing Wang, Shengli Ji, Zhe Han, Xinzhe Zhao, and Siqi Li

Deposition from Waxy Crude Oils Flowing in Transportation Pipelines: A Numerical Study 739
 Mirco Magnini and Omar K. Matar

Simplified Layer Model for Solid Particle Clusters in Product Oil Pipelines 745
 Dongze Li, Lei Chen, Qing Miao, Gang Liu, Shuyi Ren, and Zhiquan Wang

Flow and Heat Transfer Intensification in von Karmon Swirling Flow by Sucrose-Based Polymer Solution 749
 Guice Yao, Jin zhao, and Dongsheng Wen

Renewable Energy

Performance Evaluation of Liquid Air Energy Storage with Air Purification 757
 Chen Wang, Xiaohui She, Ailian Luo, Shifang Huang, and Xiaosong Zhang

Optimization of Optical Window of Solar Receiver by Genetic Algorithm Combined with Monte Carlo Ray Tracing 773
 Xiao-Lei Li, Feng-Xian Sun, Jian Qiu, and Xin-Lin Xia

Application of the Superposition Technique in Conduction Heat Transfer for Analysing Arrays of Shallow Boreholes in Ground Source Heat Pump Systems 779
 Carlos Naranjo-Mendoza, Muyiwa A. Oyinlola, Andrew J. Wright, and Richard M. Greenough

Comparison of Direct Steam Generation and Indirect Steam Generation of Solar Rankine Cycles Under Libyan Climate Conditions 785
 Amin Ehtiwesh, C Kutlu, Yuehong Su, and Jo Darkwa

Heat Transfer in Unconventional Geothermal Wells: A Double Numerical Modelling Approach 791
 Theo Renaud, Patrick Verdin, and Gioia Falcone

An Experimental Investigation of a Thermochemical Reactor for Solar Heat Storage in Buildings 797
 Cheng Zeng, Yang Liu, Xiaojing Han, Ming Song, Ashish Shukla, and Shuli Liu

Thermal and Electrical Performance Evaluation and Design Optimization of Hybrid PV/T Systems 805
 Moustafa Al-Damook, Mansour Al Qubeissi, Zinedine Khatir, Darron Dixon-Hardy, and Peter J. Heggs

Energy conversion and storage

Investigations on the Thermophysical Properties of an Organic Eutectic Phase Change Material Dispersed with GNP-AG Hybrid Nanoparticles 817
 Neeshma Radhakrishnan and C. B. Sobhan

Thermal Analysis of a 10 Ah Sodium Sulphur Battery (NaS) Cell 823
 Ebikienmo E. Peters, Peter J. Heggs, and Darron W. Dixon-Hardy

The Effect of Air Distribution Modes and Load Operations on Boiler Combustion 827
 Yingai Jin, Cong Tian, Yaohong Xing, Mingyu Quan, Jiwei Cheng, Yuying Yan, and Jiatong Guo

Transient Performance Improvement for Thermoelectric Generator Used in Automotive Waste Heat Recovery 833
 Kuo Huang, Yuying Yan, Guohua Wang, Bo Li, and Adeel Arshad

Heat Transfer Analysis of a Liquid Piston Gas Compressor 839
 M. Kaljani, Y. Mahmoudi, A. Murphy, J. Harrison, and D. Surplus

Progress with Development of FASTT Technology 845
 W. D. Alexander

A Numerical Model with Experiment Validation for the Melting Process in a Vertical Rectangular Container Subjected to a Uniform Wall Heat Flux 853
 M. Fadl and P. C. Eames

Experimental Study on Heat Transfer Performance of Active Magnetic Regenerator Working at Room Temperature 857
 Georges El Achkar, Bin Liu, Qi Wang, Aiqiang Chen, and Rachid Bennacer

Thermodynamic Analysis of Multi-stage Compression Adiabatic Compressed Air Energy Storage System 863
 Lixiao Liang, Jibiao Hou, Xiangjun Fang, Ying Han, Jie Song, Le Wang, Zhanfeng Deng, Guizhi Xu, and Hongwei Wu

Performance of Triangular Finned Triple Tubes with Phase Change Materials (PCMs) for Thermal Energy Storage 869
Yan Yang, Xiaowei Zhu, Hongbing Ding, and Chuang Wen

Thermal Analysis of an Earth Energy Bank 875
Muyiwa A. Oyinlola, Carlos Naranjo-Mendoza, Sakellariou Evangelos, Andrew J. Wright, and Richard M. Greenough

Numerical Study on Charging Process of Latent Thermal Energy Storage Under Fluctuating Thermal Conditions 879
Zhi Li, Yiji Lu, Xiaoli Yu, Rui Huang, and Anthony Paul Roskilly

Thermal and Electrical Property of Silicon with Metastable Phases Introduced by HPT Process 883
Masamichi Kohno, Mizuki Kashifuji, Kensuke Matsuda, Harish Sivasankaran, Yoshifumi Ikoma, Makoto Arita, Shenghong Ju, Junichiro Shiomi, Zenji Horita, and Yasuyuki Takata

Micro Gas Turbine Range Extender Performance Analysis Using Varying Intake Temperature 887
R. M. R. A. Shah, M. A. L. Qubeissi, A. McGordon, M. Amor-Segan, and P. Jennings

Thermoacoustic Electricity Generator for Rural Dwellings in Developing World 893
Wigdan Kisha and David Hann

Heat Transfer Within PCM Heat Sink in the Presence of Copper Profile and Local Element of the Time-Dependent Internal Heat Generation 899
Nadezhda S. Bondareva and Mikhail A. Sheremet

Effects of Bionic Models with Simultaneous Thermal Fatigue and Wear Resistance 903
Dahui Yu, Ti Zhou, Hong Zhou, Haiqiu Lu, Haifeng Bo, and Yuying Yan

Experimental Study and Sensitive Simulation of a Heat Pipe Photovoltaic/Thermal System 909
T. Zhang, Z. W. Yan, and H. D. Fu

Convection

Natural Convection from Heated Surface-Mounted Circular Cylinder



H. Malah, Y. S. Chumakov, and S. Ramzani Movafagh

1 Introduction

In recent years, there are more efforts on natural convection heat transfer from a horizontal cylinder, because of its practical applications. However, unconfined cylinder is well studied; the effect of introducing end-walls on the heat transfer rate of cylinder is considerably less investigated [1]. By development of computers and enhancement of advanced computational techniques, many studies of flow over a bluff body relevant to solid wall have been performed numerically [2], although experimental studies keep their place among researchers' efforts because of their advantages [3]. All numerical and experimental studies confirmed the expected rise on the heat transfer rate in the upstream region of the cylinder. However, the flow configuration, bluff body geometry and applied conditions on solid walls affect the arising flow [4, 5]. In this study, a numerical model of a heated horizontal circular cylinder mounted on vertical isothermal plate is employed to evaluate the natural convection heat transfer. To quantify the effect of vertical plate on the heat transfer from the cylinder surface, the aspect ratio of the cylinder (H/D) is selected equal to 0.6, in order to immerse in the arisen boundary layer on the vertical plate entirely. This geometrical configuration is evaluated on the vertical plate at fixed Grashof number equals 3×10^8 that represents laminar Grashof number. As a result, we describe the three-dimensional characteristics of natural convection heat transfer, which affect flow around the circular cylinder mounted on vertical heated plate. The results proved the significant effect of height of cylinder on the heat transfer rate from circular cylinder surface in the case of

H. Malah (✉) · Y. S. Chumakov

Institute of Applied Mathematics and Mechanics, Peter the Great St. Petersburg Polytechnic University, St. Petersburg 195251, Russian Federation

e-mail: hamid.malah@gmail.com

S. Ramzani Movafagh

Department of Environmental Engineering, Faculty of Engineering and Technology,

Saint-Petersburg State Institute of Technology, St. Petersburg 190013, Russian Federation

laminar natural convection flow. This study improves fundamental understanding of the buoyancy-induced flows around three-dimensional obstacles in different industrial applications to address the anticipated needs to enhance the rate of heat transfer and safety simultaneously.

2 Computational Methodology

In this work, in order to develop a laminar boundary layer on the heated vertical plate, the cylinder was mounted on an isothermal rectangular plate, which its dimensions considered equal to $100D$ in vertical direction (Y) and $7D$ in lateral direction (X). The vertical plate temperature is set to 333.15 K. In order to achieve a developed laminar incoming flow around the cylinder, the vertical position of cylinder from leading edge of rectangular plate is equal $30D$, which provides Grashof number for laminar flow equals to 3×10^8 . In addition, the computational domain was extended $9D$ from leading and trailing edge of plate and $10D$ normal to the plate (Z -direction) in order to ensure impermeability and slip in these regions.

In the analysed case of high aspect ratio cylinder, which performed in the similar conditions as present study, the computed thickness of incoming boundary layer on the vertical plate was equal to $0.9D$ [4]. The cylinder diameter (D) was equal to 0.02 m with fixed surface temperature at 353.15 K. The cylinder height (H) is fixed to $0.6D$, in order to immerse in the laminar boundary layer entirely.

The schematic configuration of problem, its dimensions and imposed boundary conditions are shown in Fig. 1a. In Fig. 1a, the solid walls were applied no-slip boundary condition. The boundary condition, which called ‘‘Opening’’ in Fig. 1a, refers to penetrable side of computational domain in constant pressure.

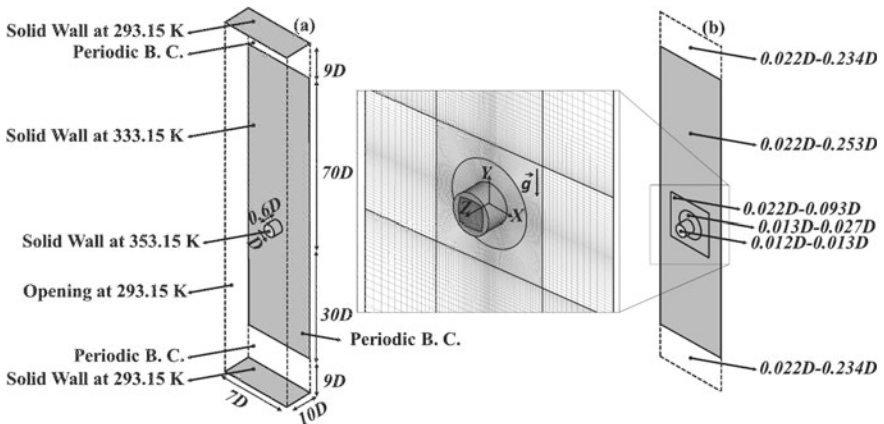


Fig. 1 Schematic of the case geometry and computational details: **a** problem configuration, **b** multi-blocked grid layout

In this work, the case geometry discretized by using body-fitted mesh. The multi-blocked grid in XY plane forms two-dimensional grid, and the range of its cells size in different region is shown in Fig. 1b. The two-dimensional grid, which consists of 41 thousand cells, was clustered to the vertical plate over Z -axis with a coefficient equals to one and generates the three-dimensional grid layout. The cells' size over Z spatial orientation is set to $0.02D$. The three-dimensional mesh grid consists of approximately 4.8 million hexahedron cells.

In this study, a time-based numerical simulation was performed by using a commercial code (ANSYS FLUENT 16.2). The numerical model is based on the momentum and the energy balance equations, which were coupled by considering the fractional step algorithm and solved by using the Boussinesq approximation. The governing equations were discretized using second-order accurate schemes for all the spatial derivatives. Lastly, the computations were run up to 300 s in physical time with a time step equal to 0.002 s.

3 Results

In this work, in order to survey on characteristics of natural convection heat transfer around surface-mounted circular cylinder, the localized Nusselt number related to angular coordinate (Nu_θ) is determined on the solid surface of circular cylinder. To aim this purpose, the spatial angular coordinates were considered as angles, on which zero angle refers to leading edge of circular cylinder on YZ plane. In order to investigate the effect of height of cylinder on the heat transfer rate, the local Nusselt numbers at different Z coordinates along height of cylinder within laminar boundary layer thickness were presented in Table 1. Table 1 illustrates the computational results

Table 1 Local Nusselt number (Nu_θ) comparison

Z/D	Source	0	30	60	90	120	150	180
0.1	Present	12.39	11.49	8.43	4.45	3.06	3.82	6.21
	[5]	12.56	11.60	8.39	4.31	5.16	10.63	7.58
0.2	Present	21.36	20.50	14.99	6.92	2.06	3.31	5.41
	[5]	21.38	20.46	14.77	6.42	4.59	5.91	3.90
0.3	Present	24.55	23.79	18.13	8.56	2.19	2.62	3.36
	[5]	24.45	23.69	17.89	8.02	3.64	4.83	3.18
0.4	Present	24.95	24.29	18.83	9.44	2.60	2.03	2.03
	[5]	24.36	23.66	18.16	8.71	2.82	3.89	3.32
0.5	Present	25.51	24.94	19.85	10.83	3.75	2.63	1.91
	[5]	23.10	22.47	17.62	9.23	2.67	2.95	3.26
0.6	Present	30.36	30.37	26.01	17.22	9.31	8.50	7.96
	[5]	21.50	20.94	16.78	9.73	3.02	2.61	3.31

at seven discrete angular coordinates on the cylinder surface. In addition, in order to investigate the effect of cylinder aspect ratio on transferred heated flow from cylinder, the computed local Nusselt numbers of the work [3], where the results of high aspect ratio cylinder were provided, are included in Table 1 for comparison.

Based on the presented values in Table 1, the local Nusselt numbers decrease from the leading edge ($\theta = 0^\circ$) to the trailing edge ($\theta = 180^\circ$) of the cylinder for each Z coordinate. In the downstream region of the cylinder ($\theta = 120^\circ$), there is a rapid decline in value of local Nusselt numbers, and after that ($\theta = 150^\circ$) the Nusselt number values experience a slight increase. Since the rate of natural convection heat transfer is proportional to the buoyancy of the fluid, the local Nusselt numbers increase along Z -axis from confined end-wall (rectangular vertical plate) to the unconfined end of circular cylinder.

Although there is a good agreement between the values of local Nusselt number in the present analysis and results of high aspect ratio study [5], Table 1 demonstrates two regions on the cylinder surface, where the rate of convection heat transfer is comparable between low and high aspect ratio cylinder. The first region is at the unconfined end of cylinder (around $Z/D = 0.6$), where incoming flow can bypass the cylinder in the case of low aspect ratio cylinder, so there is anticipated a dramatically increase in the local Nusselt numbers. The second zone is downstream region of cylinder (from $\theta = 120^\circ$ to $\theta = 180^\circ$), where the arisen heated flow from the high aspect ratio cylinder acts as a separate source of heat generation. Since the high aspect ratio cylinder crosses the formed boundary layer entirely, arisen heated flow interacts with the incoming boundary layer and leads to an obvious increase in the rate of convection heat transfer.

An overall view of the data in Table 1 demonstrates the fact that the leading edge of surface-mounted circular cylinder ($\theta = 0^\circ$) is a specific line for this problem. Although the local Nusselt number is practically constant for a long cylinder [5], the local Nusselt number increases for a short cylinder on the leading edge ($\theta = 0^\circ$) along cylinder height (Z -direction). The localized Nusselt number in the wake region of the cylinder is qualitatively similar for different variants, representing a slow, almost monotonic decrease in local Nusselt number with increasing spatial angular coordinates around the cylinder.

4 Conclusions

By comparing the numerical results of arisen convection heat transfer rate in present work (low aspect ratio) with the results of high aspect ratio cylinder [5], the significant effect of cylinder aspect ratio on the Nusselt number in the case of laminar natural convection flow is demonstrated.

Maximum values of local Nusselt number are observed at the confined end of cylinder near the vertical plate. These values are located in laminar incoming boundary layer, which arose on the heated vertical plate. Furthermore, heat transfer

coefficient decreases from leading edge of cylinder in upstream region to trailing edge in the downstream of the cylinder.

References

1. C.E. Clifford, M.L. Kimber, Optimizing laminar natural convection for a heat generating cylinder in a channel. *J. Heat Transfer* **136**, 112502 (2014)
2. G. Delibra, K. Hanjalic, D. Borello, F. Rispoli, Vortex structures and heat transfer in a wall-bounded pin matrix: LES with a RANS wall-treatment. *Int. J. Heat Fluid Flow* **31**, 740–753 (2010)
3. J.K. Ostanek, K.A. Thole, Wake development in staggered short cylinder arrays within a channel. *Exp. Fluids* **53**, 673–697 (2012)
4. H. Malah, Y.S. Chumakov, A.M. Levchenya, A study of the vortex structures around circular cylinder mounted on vertical heated plate. *AIP Conf. Proc.* **2018**, 050018 (1959)
5. Y.S. Chumakov, A.M. Levchenya, H. Malah, The vortex structure formation around a circular cylinder placed on a vertical heated plate. *St. Petersburg State Polytech. Univ. J. Phys. Math.* **11**, 56–66 (2018)

Experimental Investigation of Transitional Flow Forced Convection Heat Transfer Through a Smooth Vertical Tube with a Square-Edged Inlet



Abubakar I. Bashir, Marilize Everts, and Josua P. Meyer

1 Introduction

Limited work has been done on forced convection heat transfer in the transitional flow regime, especially in horizontal tubes with higher heat fluxes where the uncertainties are low. Forced convection experiments in horizontal tubes are challenging to perform because of the difference in density between the fluid near the surface (hot) and near the center of the tube (cold) that cause buoyancy effects and lead to mixed convection. Mixed convection can change the heat transfer characteristics in the laminar and transitional flow regimes significantly. For forced convection, the theoretical fully developed laminar flow Nusselt number is 4.36 (for a constant heat flux boundary condition). For mixed convection, the Nusselt numbers can increase up to 180–520% higher than 4.36 [1–3] due to buoyancy effects. In vertical tubes, the buoyancy effects can be reduced as the flow is in the same direction as the buoyancy force and is mostly suppressed at higher Reynolds numbers. Therefore, forced convection conditions can be achieved in the laminar and transitional flow regimes of a smooth vertical tube, even at higher heat fluxes.

Ghajar and Tam [3] found that the boundaries and the heat transfer characteristics of the transitional flow regime were inlet dependent. Everts and Meyer [1] investigated the effect of buoyancy on the heat transfer in the transitional flow regime and found that the transition Reynolds numbers were significantly affected by the buoyancy effects. Furthermore, buoyancy effects increased with increase in heating, and therefore, heating also changes the transition boundaries. However, these analyses

A. I. Bashir · M. Everts · J. P. Meyer (✉)
Department of Mechanical and Aeronautical Engineering, University of Pretoria, Pretoria 0002,
South Africa
e-mail: josua.meyer@up.ac.za

A. I. Bashir
Department of Mechanical Engineering, Bayero University, Kano, Nigeria

focused on mixed convection conditions in horizontal tubes. It is important to investigate the heat transfer characteristics for pure forced convection in the transitional flow regime in order to fundamentally understand the behavior of transition heat transfer without the influence of buoyancy. Therefore, the purpose of this study was to experimentally investigate the single-phase forced convection heat transfer characteristics of the transitional flow regime in a smooth vertical tube, with a square-edged inlet, heated at constant heat flux.

2 Experimental Setup

The schematic of the experimental facility is shown in Fig. 1 and water was used as working fluid. A magnetic gear pump was used to pump the water from a storage tank to the flow meters, flow-calming section and inlet section and then to the test section. After the test section, the heated water returned to the storage tank for cooling and recirculation. The flow-calming section was placed prior to the test section to ensure a uniform flow distribution through the inlet section and test section, because transition is inlet dependent. A square-edged inlet geometry was used for all the experiments.

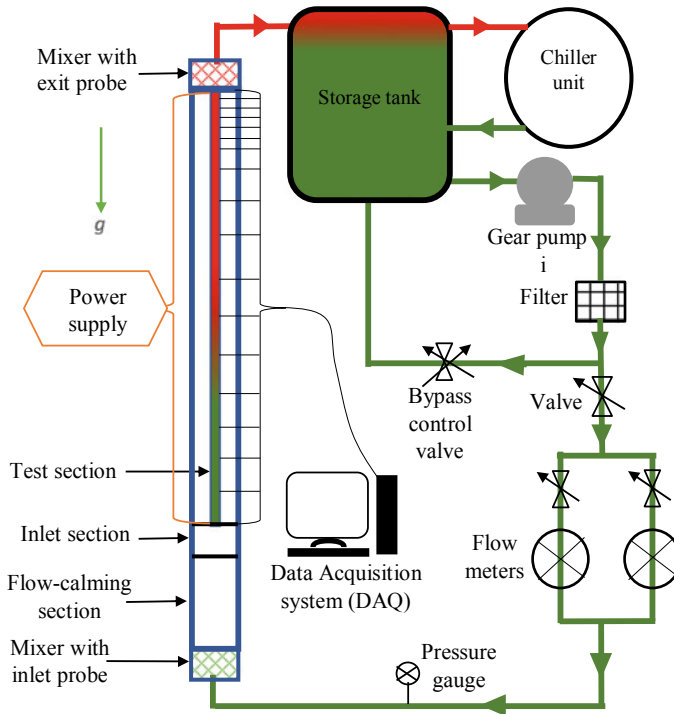


Fig. 1 Schematic of the experimental facility

The test section was a smooth hard drawn copper tube with an inner diameter of 5.1 mm and a heated length of 4.52 m (maximum length-to-diameter, x/D_i of 886). Twenty-one thermocouples were attached to the test section to measure the local wall temperatures. The inlet and exit bulk fluid temperatures were measured using two Pt100 probes placed inside the inlet and exit mixers, respectively. The test section was heated at heat fluxes of 1, 4, 6 and 8 kW/m² using a direct current (DC) power supply. At a Reynolds number of 2000, the flow was found to be fully developed from $x/D_i = 416$, because the heat transfer coefficients became relatively constant along the tube length. Therefore, the local results at $x/D_i = 592$ were used for the fully developed flow analyses. The test section was set at vertical upward flow direction to avoid the effect of buoyancy or free convection that might cause mixed convection. The experiments were performed for Reynolds numbers between 1000 and 6000 to cover the entire transitional flow regime as well as sufficient parts of the laminar and turbulent flow regimes.

The setup was validated against the literature by comparing laminar and turbulent flow heat transfer coefficients with well-known correlations. The laminar flow heat transfer results were compared using the flow regime map of Metais and Eckert [4] for constant heat flux in vertical tubes. All the heat transfer results fell within the forced convection region of the Metais and Eckert [4] map. Furthermore, at a Reynolds number of 1000, the laminar forced convection Nusselt number was 4.41, which is within 1.1% of 4.36. Thus, the forced convection condition was confirmed in the laminar flow regime up to the start of transition. In the turbulent flow regime, the maximum deviation of the heat transfer coefficients from Gnielinski [5] correlation was 3.9%.

3 Results

Figure 2a compares the local fully developed heat transfer results in terms of Nusselt number ($Nu = hD_i/k$) as a function of Reynolds number at $x/D_i = 592$. The Nusselt numbers for all the different heat fluxes in the laminar flow regime were approximately the same and approached the theoretical forced convection Nusselt number of 4.36 for a constant heat flux boundary condition. This indicated that there is negligible or no buoyancy effects and confirmed forced convection conditions for all the heat fluxes up to the start of transitional flow regime. However, as the Reynolds number increased and the flow approached the transitional flow regime, the laminar flow Nusselt numbers of all the heat fluxes increased slightly, which might be due to the effect of variable fluid property (viscosity). As expected, there was a negligible difference between the results of the different heat fluxes in the turbulent flow regime, therefore, the flow was also dominated by forced convection conditions. Because both the laminar and turbulent flow regimes were dominated by pure forced convection heat transfer, it confirmed that the entire transitional flow regime was also dominated by forced convection.

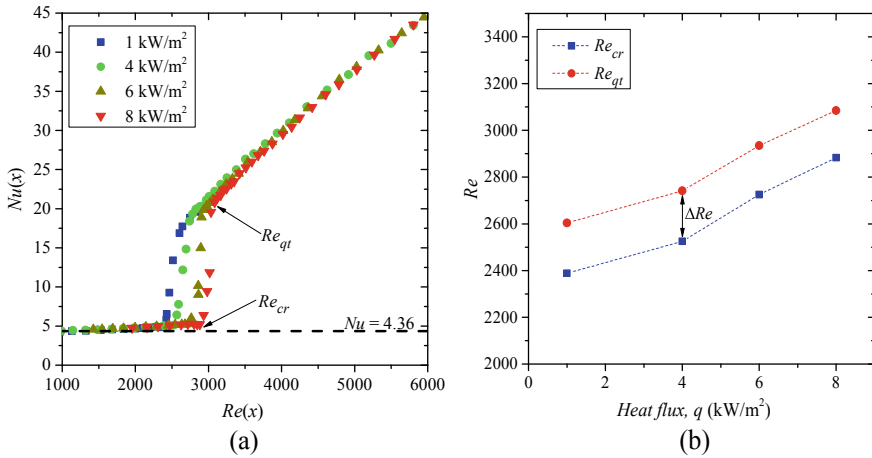


Fig. 2 Comparison of **a** fully developed local Nusselt numbers as a function of Reynolds numbers at $x/D = 592$ for the different heat fluxes and **b** Reynolds numbers at the start (Re_{cr}) and end (Re_{qt}) of transitional flow regime in **a** as a function heat flux

For all the heat fluxes in Fig. 2a, transition occurred at the same mass flow rate of approximately 0.00890 kg/s, while the critical Reynolds numbers at the start of transition increased with increase in heat flux. As the heat flux was increased for a constant mass flow rate, the increased fluid temperature led to a decreased viscosity which in turn caused the Reynolds numbers to increase. At a heat flux of 1 kW/m², transition occurred at a critical Reynolds number of 2388, while at 8 kW/m², the critical Reynolds number increased to 2883 for the same mass flow rate. Similarly, transition ended at approximately the mass flow rate but the Reynolds number at end of transition also increased with increased heat fluxes. Figure 2b compares the transition Reynolds numbers for the different heat fluxes in Fig. 2a. It followed that both the Reynolds numbers at the start (Re_{cr}) and end (Re_{qt}) of the transitional flow regime increased simultaneously with increasing heat flux. It also showed that the width of the transitional flow regime, defined by Everts and Meyer [1] as $\Delta Re = Re_{cr} - Re_{qt}$, for all the heat fluxes was approximately equal and ranged between 203 and 219. This is different from that of mixed convection condition as was found by Evert and Meyer [1] in horizontal tubes. For mixed convection condition, the width of the transitional flow regime was significantly affected by free convection effects and therefore decreased with increasing heat flux.

4 Conclusions

Single-phase forced convection heat transfer characteristics of the transitional flow was experimentally investigated using a smooth vertical tube with a square-edged